ELSEVIER

PII: S0032-3861(96)00716-1

Polymer Vol. 38 No. 8, pp. 1929–1944, 1997

0032-3861/97/$17.00+0.00

Quantitative model for the time development of diffusion-limited oxidation profiles

J. Wise, K. T. Gillen* and R. L. Clough
Sandia National Laboratories, Albuquerque, NM 87185-1407, USA
(Received 11 January 1996; revised 17 June 1996)

We combine diffusion and kinetic expressions with chemical/mechanical property relationships to develop a complete, quantitative model with no arbitrarily adjustable parameters for the time development of diffusion-limited oxidation profiles. Excellent agreement between experimental and theoretical modulus profiles for two materials (a nitrile and a neoprene) confirms our understanding of diffusion-limited oxidation and its time and temperature dependencies. The simple assumption of no time dependencies in any of the model parameters is adequate for predictions relevant to elastomer service lifetimes. © 1997 Elsevier Science Ltd. All rights reserved.

(Keywords: diffusion-limited oxidation; ageing; profile)

INTRODUCTION

Diffusion-limited oxidation (DLO) is frequently a significant influence on reactive systems in which oxygen diffuses into a solid, and can be observed when the rate of oxygen consumption within the material is greater than the rate at which oxygen can be resupplied to the interior of the material by diffusion. Typical diffusion-limited oxidation effects are shown in *Figures 1* and *2*. These figures show modulus profiles[1,2] at selected times and temperatures for a nitrile rubber in the range 65–125°C and for a neoprene rubber in the range 100–150°C, respectively. (The solid curves in the figures are predictions resulting from the modelling described in this work and are fully discussed later in the paper.) Considerable complexity of the profiles with respect to both time and temperature is evident. At the higher temperatures, profiles are heterogeneous at all times, with the extent of heterogeneity increasing with time; at the lower temperatures, profiles remain homogeneous for long times.

We have noted that thermo-oxidative ageing of elastomers typically results in heterogeneities[3]. Indeed, heterogeneities resulting from diffusion limitations are common; a well-known example of such effects pertains to reaction on porous catalysts[4]. Potential problems arise whenever it is assumed that oxidation is homogeneous when, in fact, it is heterogeneous. One such problem that we have shown[5] is the apparent contradiction between the ageing behaviours of ultimate tensile elongation and ultimate tensile strength resulting from diffusion-limited oxidation. Another potential problem arises with regard to predictions of polymer service lifetimes, which are commonly made by extrapolating the results of high-temperature, accelerated tests to service temperatures. Among the many hazards inherent to this approach are those stemming from DLO. Because of the economic importance of accurate lifetime predictions, a thorough understanding of DLO effects is clearly needed.

We have presented a qualitative picture of the development (in elastomers) of enhanced heterogeneity with time[3]: Because increasing oxidation leads to hardening (net cross-linking) and, consequently, reduced permeabilities, all oxygen concentration profiles are expected to become accentuated with time. That is, greater oxidation near the air-exposed surfaces relative to the interior regions results in reduced permeability near the surfaces, which, in turn, leads to further reductions in oxygen concentration in the interior of the material relative to the surfaces. Subsequent oxidation is therefore increasingly localized near the air-exposed surfaces through a positive-feedback mechanism. A more complete understanding reveals that the reduction in permeability is not necessary for the formation of heterogeneities: through time, small heterogeneities can grow into large heterogeneities even if permeability remains constant.

In this report, we present a rigorous mathematical formalism of the above-described picture. Using diffusion and kinetic expressions and chemical/mechanical property relationships, we develop a complete, quantitative model with no arbitrarily adjustable parameters for the time-development of modulus profiles. With this model, we demonstrate that DLO can fully explain the observed profiles.

EXPERIMENTAL

Compression-moulded sheets (~2 mm thick) of a typical commercial nitrile rubber formulation (100 parts of Hycar 1052 resin, 65 pph of N774 carbon black, 15 pph of Hycar 1312, 5 pph of zinc oxide, 1.5 pph of 2246 (hindered phenol) antioxidant, 1.5 pph of sulfur, 1.5 pph of MBTS (2,2′-benzothiazyl disulphide), 1 pph of stearic

* To whom correspondence should be addressed

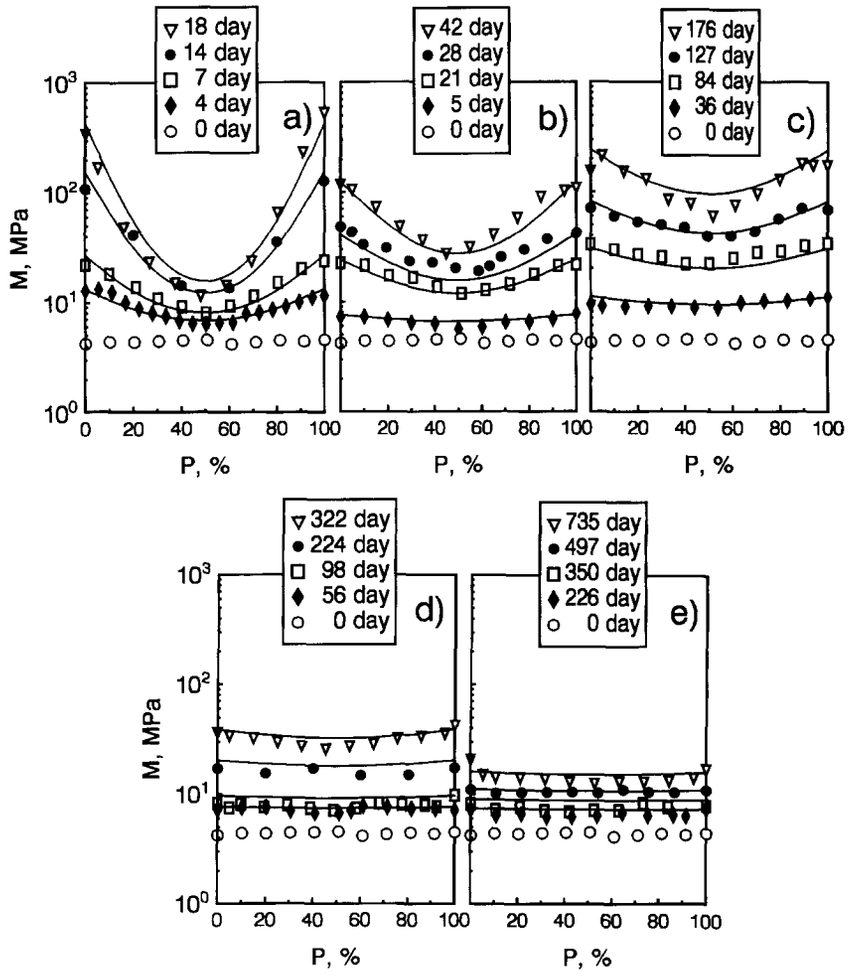

Figure 1 Modulus profiles as functions of time for 0.2 cm thick nitrile rubber samples following thermal ageing in air at: (a) 125°C, (b) 110°C, (c) 95°C, (d) 80°C and (e) 65°C. *P*, percentage of distance from one air-exposed surface to the opposite air-exposed surface. The lines represent predictions of time-dependent profiles assuming permeability remains constant at its initial (temperature-dependent) value

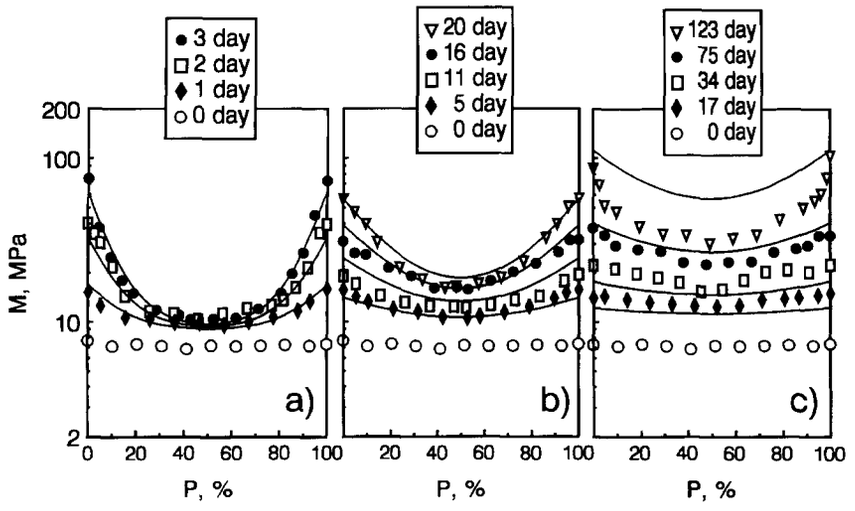

Figure 2 Modulus profiles as functions of time for 0.22 cm thick neoprene rubber samples following thermal ageing in air at: (a) 150°C, (b) 120°C and (c) 100°C. The lines represent predictions of time-dependent profiles assuming permeability remains constant at its initial value

acid) and of a typical commercial neoprene rubber formulation (100 parts of Neoprene GN, 60 pph of hard clay, 5 pph of zinc oxide, 4 pph of magnesia, 2 pph of 2246 antioxidant, 0.5 pph of stearic acid) were obtained from the Burke Rubber Co.

Strips approximately 6 mm wide and 150 mm long were cut from the rubber sheets and aged in air-circulating ovens (±1°C stability). Modulus profiles with a spatial resolution of ~50 μm were obtained on sample cross-sections using an instrument that has been

described in detail elsewhere[1,2]. This instrument measures inverse tensile compliance, a quantity closely related to tensile modulus. Oxygen consumption rates were measured using a technique that has also been described in detail elsewhere[5]. This technique involves chromatographic quantitation of the change in oxygen content caused by reaction with polymer in sealed containers over a known time interval. Oxygen permeability and diffusion measurements were performed on an Oxtran-100 coulometric permeation apparatus (Modern Controls, Inc., Minneapolis, MN, USA), which is based on ASTM standard D3985-81. Several modifications, the most important of which was placing the sample holder in an oven, had been made to this instrument to permit data acquisition at temperatures up to ~100°C.

THEORY

DLO describes a situation in which there is competition between diffusion of and reaction with oxygen. Accordingly, study and modelling of DLO requires models for both oxygen diffusion and oxidation kinetics. To model diffusion we use Fick's law; to model the oxidation kinetics we begin with the basic autoxidation scheme (BAS)[6,7], a long-used and widely accepted kinetic scheme for autoxidation of organic materials. The BAS involves bimolecular termination reactions of the radical chain carriers. This is not, however, a realistic model for thermo-oxidative degradation of stabilized materials because stabilized materials are expected to undergo unimolecular termination (more properly, pseudo-first-order termination by reaction with antioxidant). In addition, chain branching via hydroperoxide decomposition should be significant at elevated temperatures. Thus, we base our analysis of polymer oxidation on the variant of the BAS shown in *Scheme 1*. For this kinetic scheme, the oxygen consumption rate, ϕ, under steady-state conditions (i.e. $d[R\cdot]/dt = d[ROO\cdot]/dt = d[RO\cdot]/dt = d[HO\cdot]/dt = 0$) is

$$\phi = \frac{d[O_2]}{dt} = \frac{C_1[O_2]}{1 + C_2[O_2]} \tag{1}$$

where

$$C_1 = \frac{k_1 k_2}{k_5} \qquad C_2 = \frac{k_2(k_4 - 2k_3)}{k_5(k_3 + k_4)} \tag{2}$$

and $k_3 = k_3'[RH]$. The functional form of equation (1) is identical to that derived for other common BAS variants, including unimolecular termination in the absence of ROOH decomposition, and bimolecular termination (also in the absence of ROOH decomposition) using the standard simplifying assumptions of long kinetic chain length and specific ratio of (bimolecular) termination constants[8]. Modelling based on the functional form of equation (1) should therefore be quite general.

A useful relation[9] obtained by multiplying both sides of equation (1) by the quantity L^2/pP_{ox} is

$$\frac{\phi_0 L^2}{pP_{ox}} = \frac{\alpha_0}{1 + \beta_0} \tag{3}$$

where ϕ_0 is the oxygen consumption rate under ambient equilibrium (non-DLO) conditions, L is the sample thickness, p is the oxygen partial pressure surrounding the sample and P_{ox} is the oxygen permeability of the sample (= DS, the product of the oxygen diffusivity and oxygen solubility). The parameters α_0 and β_0 are given by

$$\alpha_0 = \frac{C_1 L^2}{D} \qquad \beta_0 = C_2[O_2]_0 = C_2 Sp \tag{4}$$

where p is the oxygen partial pressure above the sample, $[O_2]_0$ is the dissolved oxygen concentration (= Sp, from Henry's law) at the sample surface (in equilibrium with the surrounding atmosphere), and C_1 and C_2 are given in equation (2). The utility of equation (3) arises from the fact that all of the physical quantities on the left-hand side as well as β_0 on the right-hand side are measurable, allowing α_0 to be calculated directly. (The parameter β_0 is conveniently measured indirectly using the relation

$$\frac{\phi_1}{\phi_0} = \frac{1 + \beta_0}{p_0/p_1 + \beta_0} \tag{5}$$

which follows from equation (1) and the definition of β_0 in equation (4). See the discussion in Wise *et al.*[5].

Briefly, our solution to the problem of the time development of profiles is a stepwise procedure in which the time dependence is introduced through a series of sequential solutions, denoted by step counter i, with each step of time interval τ. We begin the solution to the time-dependent profile at step $i = 0$ by establishing boundary and initial ($t = 0$) conditions, and then solve the continuity equation to obtain an oxygen concentration profile. A cumulative oxidation profile is calculated from the oxygen concentration profile as a summation with respect to time. A modulus profile is calculated from the cumulative oxidation profile and subsequently used to calculate changes in oxygen permeability, thus redefining 'initial' conditions appropriate to the time interval from $i\tau$ to $(i + 1)\tau$. A new oxygen concentration profile is calculated from the continuity equation and the process is repeated. This scheme is now described in detail.

For constant diffusivity (with respect to position) and Fickian diffusion, the non-dimensionalized time-independent continuity equation[9] is

$$\frac{\partial^2 \theta}{\partial X^2} = \frac{\alpha_0 \theta}{1 + \beta_0 \theta} \tag{6}$$

$$\begin{aligned}
\text{polymer} &\xrightarrow{k_1} \text{R}\cdot \\
\text{R}\cdot + \text{O}_2 &\xrightarrow{k_2} \text{ROO}\cdot \\
\text{ROO}\cdot + \text{RH} &\xrightarrow{k_3'} \text{ROOH} + \text{R}\cdot \\
\text{ROO}\cdot &\xrightarrow{k_4} \text{products} \\
\text{R}\cdot &\xrightarrow{k_5} \text{products} \\
\text{ROOH} &\xrightarrow{k_6} \text{RO}\cdot + \cdot\text{OH} \\
\text{RO}\cdot + \text{RH} &\xrightarrow{k_7} \text{ROH} + \text{R}\cdot \\
\text{HO}\cdot + \text{RH} &\xrightarrow{k_8} \text{HOH} + \text{R}\cdot
\end{aligned}$$

Scheme 1

where

$$X = x/L \qquad \theta = [O_2]/[O_2]_0 \tag{7}$$

are the dimensionless position and concentration variables, respectively. It is important to realize that Fickian diffusion refers implicitly to isotropic materials, in which solubility does not vary with position[10]. Having explicitly assumed constant diffusivity in equation (6), it is understood that we are now developing a model in which $P_{ox}(= DS)$ is time- and position-independent. The more general cases of equation (6), in which P_{ox} varies, are developed and discussed in later sections.

The interval X is divided into k segments δX, each of length $1/k$, giving $k+1$ points $j\,\delta X$ with $j = 0, 1, 2, \ldots, k$. We used $k = 100$ in this work. To calculate the profile θ_j, the following set of $k-1$ simultaneous equations[9] was formulated as a solution to equation (6):

$$\theta_{j-1} = \frac{\alpha_0 \theta_j (\delta X)^2}{1 + \beta_0 \theta_j} + 2\theta_j - \theta_{j+1} \tag{8}$$

with $j = 1, 2, 3, \ldots, k-1$; the values of θ_0 and θ_k are boundary conditions. (For our samples with two air-exposed surfaces, $\theta_0 = \theta_k = 1$.) The set of equations (8) permits straightforward numerical solution to the profile θ_j by starting the calculation with boundary condition θ_k and choosing trial values of θ_{k-1} until consistency with boundary condition θ_0 is achieved.

After obtaining the oxygen concentration profile (θ_j) calculated as the solution to the continuity equation (equation (6)), we use these values to calculate the normalized (to the sample surface) oxidation rate U_j at each position within the sample:

$$U_j \equiv \frac{\phi_j}{\phi_0} \tag{9}$$

When the oxidation kinetics are time-independent (and therefore position-independent) (i.e. $C_{1_j} = C_{1_0}$ and $C_{2_j} = C_{2_0}$), it follows that

$$U_j = \left(\frac{C_{1_j}[O_2]_j}{1 + C_{2_j}[O_2]_j}\right)\left(\frac{1 + C_{2_0}[O_2]_0}{C_{1_0}[O_2]_0}\right) = \frac{\theta_j(1+\beta_0)}{1+\beta_0\theta_j} \tag{10}$$

The (relative) extent of reaction occurring in time τ at position j within the sample is given by $U_j\tau$. Thus, the cumulative (normalized) oxidation $V_j(t_m)$ at position j within the sample at time $t = m\tau$ is the summation

$$V_j(t_m) = \sum_{i=1}^{m} \frac{\phi_j(t_i)}{\phi_0}\tau = \sum_{i=1}^{m} \frac{\phi_{j,i}}{\phi_0}\tau = \sum_{i=1}^{m} U_{j,i}\tau \tag{11}$$

We use the notation $V_j(t_i)$ and $V_{j,i}$ equivalently; for clarity, we use the dual-subscript form on the right-hand sides of equations.

To connect the theoretically derived oxidation profiles with experimental results, a relationship between the experimental variable and the amount of oxidation is needed. In this work, we monitor oxidation profiles through the use of inverse tensile compliance profiles, which we commonly refer to as modulus profiles[1]. (In our previous papers, we have denoted modulus as D^{-1}. In this work, to avoid confusion with diffusivity (or reciprocal diffusivity) we denote modulus as M.) Thus, we treat the modulus (M) as a generic function of cumulative oxidation:

$$M_j(t_i) = M_0 f_1(V_{j,i}) \tag{12}$$

Conceptually, we expect that the functional form appropriate to equation (12) will be a weighted average between the two extremes of purely oxidative ageing and purely non-oxidative ageing. Such a weighting accounts for the varying degree of oxidation within the sample and reflects the fact that all degradation chemistry occurs as a result of the initiation step (rate constant k_1) of the BAS. That is, radicals ultimately react either with oxygen, to form oxidative degradation products, or without oxygen, to form non-oxidative degradation products. For the two materials examined in this work, the specific functional form of equation (12) appropriate to the data approximates an exponential. This empirical observation of exponential behaviour should not, however, be assumed to be universal.

When exponential behaviour is appropriate to the limiting cases of infinite oxygen pressure and zero oxygen pressure, a generalized relationship between modulus and cumulative oxidation at time interval m is

$$M_j(t_m) = M_0 \exp\left[\sum_{i=1}^{m}\left(\frac{\phi_{j,i}}{\phi_\infty}\right)k_{ox}\tau + \sum_{i=1}^{m}\left(1 - \frac{\phi_{j,i}}{\phi_\infty}\right)k_{nox}\tau\right] \tag{13}$$

where k_{ox} and k_{nox} are constants relating modulus to cumulative oxidation under conditions of purely oxidative ageing (infinite oxygen pressure) and purely non-oxidative ageing (zero oxygen pressure), respectively, and ϕ_∞ is the oxygen consumption rate under infinite oxygen pressure. When the oxidation kinetics are independent of time, equation (13) can be rewritten as

$$M_j(t_m) = M_0 \exp\left[\sum_{i=1}^{m}\left(\frac{\beta_0\theta_{j,i}}{1+\beta_0\theta_{j,i}}\right)k_{ox}\tau + \sum_{i=1}^{m}\left(\frac{1}{1+\beta_0\theta_{j,i}}\right)k_{nox}\tau\right] \tag{14}$$

It is important to recognize that oxidation at the sample surfaces, where $\theta = 1$, is described not by k_{ox} but rather by k_{air}:

$$k_{air} \equiv \left(\frac{\beta_0}{1+\beta_0}\right)k_{ox} + \left(\frac{1}{1+\beta_0}\right)k_{nox} \tag{15}$$

That is,

$$M_0(t) \equiv M_0 \exp(k_{air}t) = M_0 \exp(k_{air}V) \tag{16}$$

because, at the surface, $U \equiv 1$, which implies that $V = t$. Using the definitions of U (equation (9)) and k_{air} (equation (15)), equation (14) can be rewritten as

$$M_j(t_i) = M_0 \exp[k_{air}V_{j,i} + k_{nox}(t_i - V_{j,i})] \tag{17}$$

While equation (14) shows explicitly the weighting between oxidative and non-oxidative ageing, equation (17) shows more clearly the relation between modulus and cumulative oxidation. Note that k_{ox} and k_{nox} both refer to limiting pressure conditions and that, by definition, neither is pressure-dependent. It follows from equations (1) and (2) and the definition of β_0 (equation (4)) that the non-oxidative component denoted by k_5 in the BAS disappears only when $\beta_0 \gg 1$. Therefore, k_{air} (equation (15)) determined from surface modulus results in air will typically include both oxidative and non-oxidative components. We expect

this treatment using k_{ox} and k_{nox} to relate cumulative oxidation to the experimental degradation variable to be applicable to modelling of other mechanical and also chemical properties, although the functional form appropriate to these other properties may not be exponential.

In general, as the modulus of a material changes due to cross-linking and scission chemistries, the oxygen permeability ($P_{ox} = DS$) will change. Because D and S are contained in the parameters α and β, respectively (equation (4)), these potential changes require introduction of the generic functional relations

$$\alpha_j(t_i) = \alpha_0 f_2(M_{j,i}) \qquad \beta_j(t_i) = \beta_0 f_3(M_{j,i}) \quad (18)$$

We include provisions to change both α and β because we cannot assume *a priori* that changes in permeability are due solely to changes in D or solely to changes in S. Once the functional forms for equation (18) are specified, profiles reflecting changes in α and β due to oxidation are calculated. These new α and β profiles are then used to calculate a new θ profile from equation (6), and the process is repeated. The overall procedure for the most general calculation scheme is outlined in *Table 1*.

Under our current assumptions of constant diffusivity and solubility, the functionalities of equation (18) reduce to the trivial identities

$$\alpha_j(t_i) = \alpha_0 \qquad \beta_j(t_i) = \beta_0 \quad (19)$$

It is because of this simplification that there is no time dependence in equation (8). The choice of appropriate functional forms for equation (18) when diffusivity and/or solubility are not constant is non-trivial and adds considerable complexity to the derivation of the most rigorous solutions; this issue is discussed in detail later. As will be evident in the following discussions, however, this added level of complexity may be unnecessary because the much simpler time-independent solutions often do an excellent job of predicting the DLO effects.

RESULTS AND DISCUSSION

From the procedure for calculating the time development of modulus profiles summarized in *Table 1*, we see that knowledge of α_0, β_0, ϕ, L, p, P_{ox}, k_{air} (or k_{ox}) and k_{nox} with respect to time and temperature will be necessary to avoid the use of any arbitrarily adjustable parameters. Using equation (3) at a given time and temperature, α_0 can be calculated with knowledge of the parameters β_0, ϕ, L, p and P_{ox}. The parameters L and p are treated as constants because they are easily controlled experimentally. Thus, we need experimental data for ϕ, β_0, P_{ox}, k_{air} and k_{nox} as functions of both time and temperature.

It is important to recognize that the parameters β_0, ϕ and k_{air} are pressure-dependent. Any modelling using these parameters must, obviously, draw on a consistent set of data. That is, all pressure-dependent data must be adjusted to a common reference pressure. Because we are modelling modulus profiles resulting from ageing in Albuquerque, all pressure-dependent parameters in this work refer to Albuquerque ambient conditions (13.2 cmHg O_2).

Table 1 Solution scheme at each time increment for the time development of modulus profiles

Calculated profile	Equation
Oxygen concentration (θ_j)	(8)
Relative oxidation rate (U_j)	(9)
Cumulative oxidation (V_j)	(11)
Modulus (M_j)	(17)
Diffusivity (α_j)	(18)
Solubility (β_j)	(18)

Nitrile rubber: data

We have previously discussed ϕ for the nitrile rubber as a function of both time and temperature[5]; these results are reproduced in *Figure 3*. As discussed by Wise *et al.*[5], these data represent equilibrium (non-DLO) conditions. Although the results shown indicate that ϕ decreases slightly with increased ageing, this decrease is sufficiently small that we can treat ϕ as constant. The temperature dependence of ϕ over the range 65–96°C can be well described by the Arrhenius relation

$$\phi = A \exp(-E_a/RT) \quad (20)$$

with $A = 300\,\text{mol g}^{-1}\,\text{s}^{-1}$ and $E_a = 20.8\,\text{kcal mol}^{-1}$. This value of E_a is consistent with our previous measurements of E_a for this material[5], and we therefore use this relationship to extrapolate ϕ to 110 and 125°C.

We also showed[5] that the dependence of β_0 for the nitrile rubber on temperature (reproduced in *Figure 4*) can be well described by the Arrhenius relation (equation (20)) with $A = 0.0275$ and $E_a = 2.7\,\text{kcal mol}^{-1}$. Again, we use this relationship to extrapolate β_0 to 125°C. We have attempted to measure β_0 for the nitrile rubber as a function of ageing at 96°C. As shown in *Figure 5*, β_0 is constant in the early stages of ageing, although there is an indication that it may decrease by ~50% in the later stages of ageing. There are, however, large errors associated with β_0; as previously discussed[5], these errors arise from the functional form of the equation used to calculate β_0 and the conditions under which the experiments were run. As a corollary to the large errors, however, it follows that ϕ is not a sensitive function of β_0, and we therefore treat this parameter as time-independent, as indicated by the dashed line in *Figure 5*.

We model P_{ox} with implicit rather than explicit time

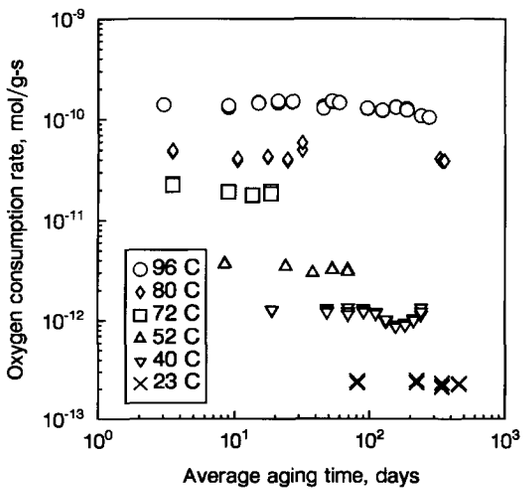

Figure 3 Oxygen consumption rates for the nitrile rubber as functions of time at the indicated temperatures

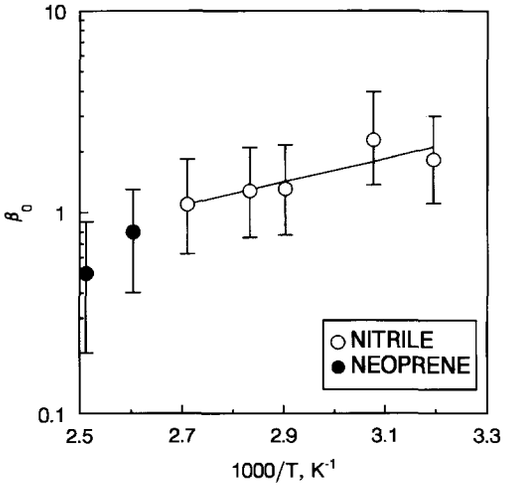

Figure 4 The parameter β_0 for the nitrile rubber (open circles) and neoprene rubber (solid circles) as a function of temperature

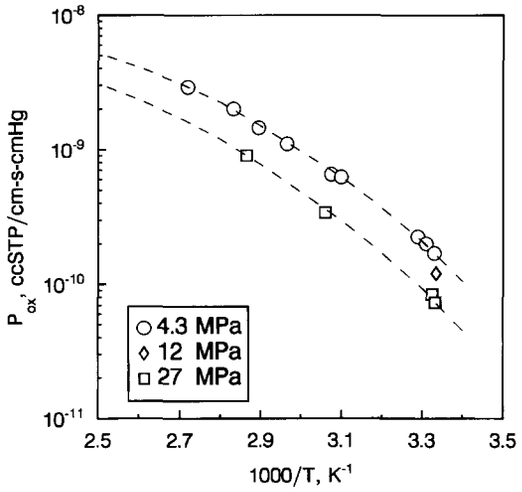

Figure 6 Oxygen permeability of the nitrile rubber as a function of temperature for the indicated values of effective modulus

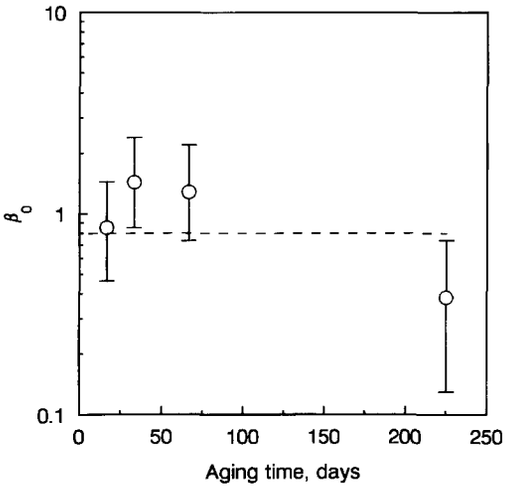

Figure 5 The parameter β_0 for the nitrile rubber as a function of time at 96°C

dependence. That is, we model P_{ox} (actually, α and β) as a function of modulus (equation (18)) and, in turn, modulus as a function of time (equation (14)). This means that we need data for P_{ox} as a function of temperature and modulus rather than as a function of temperature and time. *Figure 6* is an Arrhenius plot of the oxygen permeability of the nitrile rubber as a function of temperature for the indicated modulus values ($M_0 = 4.3$ MPa for the unaged material). Curvature of the data (non-Arrhenius behaviour) is evident. Such behaviour is often observed for permeation in elastomers[11,12], and has theoretical justification based on free volume considerations[13]. Permeation rates increase with temperature, eventually exceeding the limit measurable with our instrumentation; for the nitrile rubber we cannot reliably measure permeabilities at temperatures above ~95°C. Accordingly, we have extrapolated permeabilities of the unaged nitrile rubber to 125°C by extending the curvature observed in the 23–95°C range (upper curve in *Figure 6*). There is also evidence that P_{ox} decreases slightly as modulus increases. Treatment of the permeability/modulus dependence is complex and is discussed in detail later. For now, we assume that P_{ox} (at a given temperature) remains constant at its initial value.

Finally, to calculate modulus as a function of time (equation (17)), we need to evaluate the constants k_{air} and k_{nox}. We obtain k_{nox} by ageing nitrile rubber samples in sealed containers backfilled with nitrogen. Modulus profiles of the aged nitrile samples at the indicated times and temperatures are shown in *Figures 7a* and *7b*. In *Figure 7*, the moduli of the unaged materials are somewhat larger than in *Figures 1* and *2*. This is because the measurements in *Figure 7* were made approximately 3 years later than those in *Figures 1* and *2* and the materials had cured slightly (modulus increase) in the interim. In all cases, the modulus profiles of these non-oxidatively aged samples are essentially homogeneous. There is a small initial change upon nitrogen ageing (probably not due to dissolved oxygen; samples were pumped to remove dissolved gases), but continued ageing has no further effect. Because of the arbitrary nature of an exponential (equation (17)) fit to these modulus/time data, we instead set $k_{nox} = 0$ and treat the change in modulus due to non-oxidative ageing as a step change, ΔM_{nox}, of magnitude ~0.5 MPa for the nitrile rubber. We thus rewrite equation (17) as

$$M_j(t_i) = M_0 \exp(k_{air} V_{j,i}) + \Delta M_{nox} \qquad (21)$$

The parameter k_{air} is evaluated by fitting surface modulus data for the nitrile rubber as a function of time, at the temperatures given in *Figure 8*, to equation (21) (or equation (16)). The lack of significant deviations from the fitted lines in *Figure 8* indicates that k_{air} is time-independent. This experimental observation is consistent with the assumption of constant k_{air} implicit in equation (14).

Values of all parameters used for the time-dependent modelling of the nitrile rubber are summarized in *Table 2*.

Neoprene rubber: data

We have previously discussed ϕ for the neoprene rubber as a function of both time and temperature[5]; these results are reproduced in *Figure 9*. As for the nitrile rubber, these data also represent equilibrium (non-DLO) conditions. The increases in ϕ observed at longer times (after the oxidative induction time) correspond to severe

Table 2 Measured values of parameters for the time-dependent modelling of the nitrile rubber. $p = 13.2$ cmHg O_2 (ambient partial pressure of O_2 in Albuquerque); $L = 0.2$ cm (typical); $M_0 = 4.3$ MPa; $\rho = 1.18\,g\,cm^{-3}$

T (°C)	k_{air} (day^{-1})	ΔM_{nox} (MPa)	P_{ox} ($ccSTP\,cm^{-1}\,s^{-1}\,cmHg^{-1}$)	ϕ ($mol\,g^{-1}\,s^{-1}$)	β_0	n	b
125	2.55×10^{-1}	0.5	5.2×10^{-9}[a]	1.1×10^{-9}[a]	0.84[a]	−0.28[a]	−0.0231[a]
110	7.98×10^{-2}	0.5	4.1×10^{-9}[a]	4.1×10^{-10}[a]	0.95[a]	−0.30[a]	−0.0246[a]
95	2.29×10^{-2}	0.5[a]	2.9×10^{-9}	1.4×10^{-10}	1.10	−0.33[a]	−0.0264[a]
80	6.81×10^{-3}	0.5[a]	2.0×10^{-9}	4.0×10^{-11}	1.29	−0.35[a]	−0.0282[a]
65	1.68×10^{-3}	0.5[a]	1.2×10^{-9}	1.1×10^{-11}	1.53	−0.37[b]	−0.0302[b]
40	1.17×10^{-4}[a]	0.5[a]	4.0×10^{-10}	1.0×10^{-12}	2.11	−0.42[b]	−0.0340[b]

[a] Extrapolated
[b] Interpolated

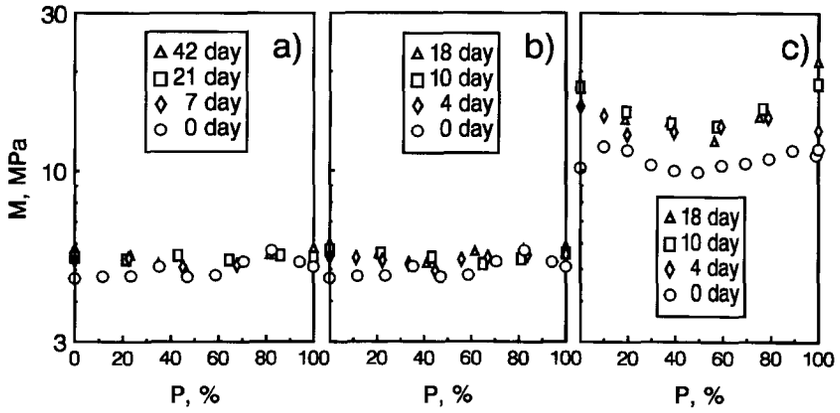

Figure 7 Effect of nitrogen ageing on: (a) nitrile rubber at 100°C; (b) nitrile rubber at 125°C; and (c) neoprene rubber at 125°C. Homogeneous step changes in modulus (ΔM_{nox}) of ~0.5 MPa for the nitrile and ~5 MPa for the neoprene are observed

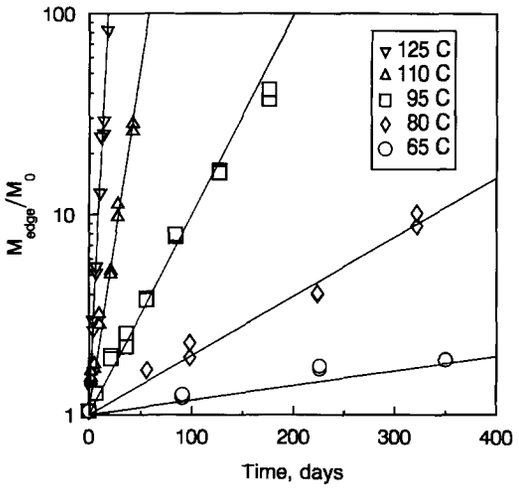

Figure 8 Surface moduli of the nitrile rubber as a function of time at the indicated temperatures. The slopes of the lines are k_{air}

mechanical degradation[5]. Because we are interested in modelling the DLO effects only before the oxidative induction time (see also the discussion of k_{air} later in this section), we can, to a good approximation, treat ϕ as time-independent. We showed[5] for this neoprene that $E_a = 21.5\,kcal\,mol^{-1}$ is appropriate to mechanical properties in the range 100–150°C and to oxygen consumption in the range 23–125°C, and therefore use this value of E_a to extrapolate ϕ to 150°C using the Arrhenius relation (equation (20)).

We have measured β_0 for the neoprene at two temperatures, as shown in *Figure 4*. These values are consistent with the general trend that $\beta_0 \sim 1$ for thermal ageing of elastomers. Because we have measurements of β_0 for the neoprene at only two temperatures and because of the large errors associated with β_0 (see discussion in Wise *et al.*[5]), it is difficult to extrapolate these data to 150°C. We therefore make the reasonable assumption that $\beta_0 = 0.6$ in the range 100–150°C, independent of temperature. We have not attempted to measure β_0 for the neoprene as a function of ageing, but by analogy to the nitrile rubber (*Figure 5*), we treat this parameter as constant with respect to time.

Figure 10 is an Arrhenius plot of the oxygen permeability of the neoprene rubber as a function of temperature for the indicated modulus values ($M_0 = 7.5$ MPa for the unaged material). Curvature of the data (non-Arrhenius behaviour) is evident, just as was observed for the nitrile rubber (see *Figure 6*). We have extrapolated permeabilities of the unaged nitrile rubber to 150°C by extending the curvature observed in the 23–80°C range (upper curve in *Figure 10*). Again, there is evidence that P_{ox} decreases slightly as modulus increases, but, again, we assume for now that P_{ox} remains constant at its (temperature-dependent) initial value.

To calculate modulus as a function of time (equation (17)), we again begin by evaluating k_{nox}. The non-oxidative ageing behaviour of the neoprene (see *Figure 7c*) is similar to that of the nitrile: there is a small initial change upon nitrogen ageing, but continued ageing has no effect (i.e. $k_{nox} = 0$). There are two ways to evaluate ΔM_{nox}. First, direct measurement by ageing the neoprene in nitrogen gives $\Delta M_{nox} \simeq 5$ MPa (see *Figure 7c*).

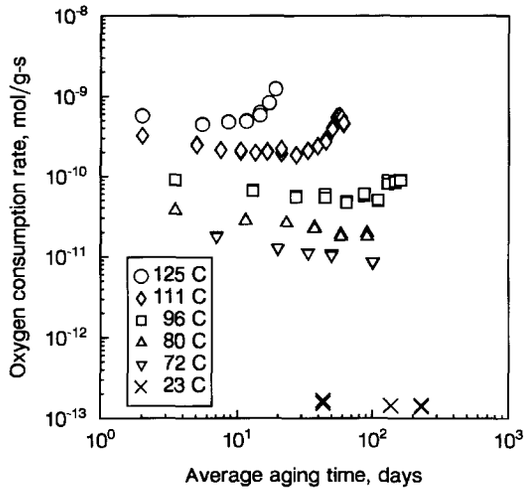

Figure 9 Oxygen consumption rates for the neoprene rubber as functions of time at the indicated temperatures

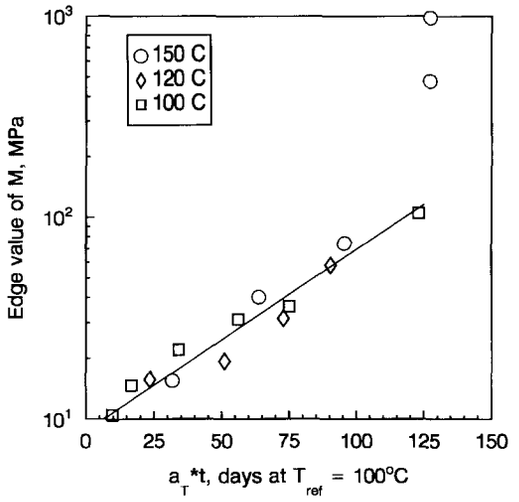

Figure 11 Empirical time/temperature superposition of the neoprene rubber surface moduli at $T_{ref} = 100°C$. The slope of the line is k_{air} at T_{ref}

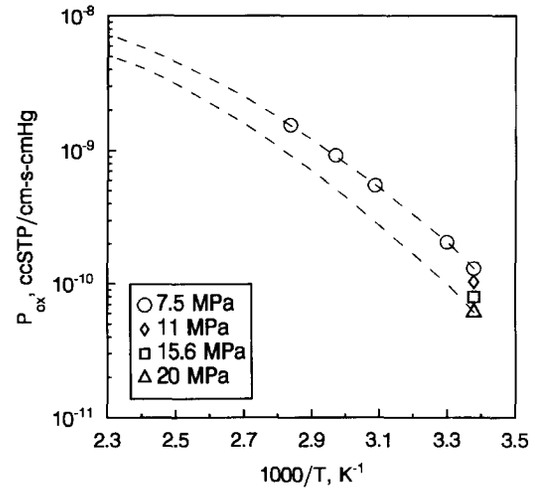

Figure 10 Oxygen permeability of the neoprene rubber as a function of temperature for the indicated values of effective modulus. Equation (37) forms the basis for the extrapolation depicted by the lower curve

Second, indirect measurement of non-oxidative ageing can be made by reference to air-aged samples if they are sufficiently heterogeneous. Such is the case for the neoprene air-aged at 150°C (see *Figure 2a*), for which ageing at the centre is virtually nonoxidative. For this sample, we find $\Delta M_{nox} \simeq 3$ MPa, consistent with the previous measurement.

To calculate k_{air}, we again analyse surface modulus data as a function of time at the various temperatures. Because the data for this material are sparse, we use the principle of time/temperature superposition to analyse all of the data simultaneously rather than attempting to analyse each temperature separately as we did for the nitrile rubber (see *Figure 8*). *Figure 11* shows the superposition of the neoprene surface modulus data at $T_{ref} = 100°C$, achieved using $a_T = 31.84$ at 150°C and $a_T = 4.52$ at 120°C, corresponding to $E_a \simeq 22$ kcal mol^{-1}. The data of *Figure 11* can be well described by

$$M(t) = 8.8 \exp(k_{air} t) \qquad (22)$$

Notice (*Figure 11*) that equation (22) is only valid for $a_T t < 125$ days; at longer times the surface modulus data deviate significantly from the fitted line. The time at which this deviation occurs is consistent with our previous measurements of the induction time for the neoprene[5], when oxidation rates increase rapidly (see *Figure 9*). This means that k_{air} at a given temperature has a corresponding maximum valid prediction time.

The fit represented by equation (22) provides a third approach to calculating ΔM_{nox}. By comparison of the measured value of $M_0 = 7.5$ MPa to the 8.8 MPa obtained by evaluating equation (22) at $t = 0$ we find $\Delta M_{nox} = 1.3$ MPa. This value is reasonably consistent with the two values of ΔM_{nox} measured and discussed earlier in this section.

Values of all parameters used for the time-dependent modelling of the neoprene rubber are summarized in *Table 3*.

Comparison with theory: time-independent

As described in the previous sections, the nitrile and neoprene data permit us to treat k_{ox}, ϕ and β_0 as constants with respect to time and to treat $k_{nox} = 0$. This leaves P_{ox} as the remaining parameter with a potential for time dependence. In *Figures 6* and *10* we saw that, in fact, permeability decreases slightly with increasing modulus; we will later quantify this relationship. For the modelling described thus far, however, we have assumed that P_{ox} is time-independent. This means that as a first, simple model of the time development of modulus profiles, we assume no time dependencies of the underlying chemical and physical parameters. Because this model assumes that permeability remains constant, when it actually decreases, we expect that the resulting predictions may overestimate oxidation in the sample centres, especially in the later stages of ageing when significant surface hardening occurs.

Figure 1 shows predicted profiles (solid curves) for the nitrile rubber under the assumption that all parameters remain constant. In general, the theoretical fits to the experimental data are excellent and confirm our basic understanding of DLO. For all temperatures, predictions at short times, before the onset of significant heterogenities, are virtually quantitative. This is because surface hardening has not yet led to important reductions in diffusivity, and the assumption of time-independent

Table 3 Measured values of parameters for the time-dependent modelling of the neoprene rubber. $p = 13.2$ cmHg O_2 (ambient partial pressure of O_2 in Albuquerque); $L = 0.22$ cm (typical); $M_0 = 7.5$ MPa; $\rho = 1.52$ g cm^{-3}

T (°C)	k_{air} (day^{-1})	Maximum prediction time (days)	ΔM_{nox} (MPa)	P_{ox} (ccSTP cm^{-1} s^{-1} cmHg^{-1})	ϕ (mol g^{-1} s^{-1})	β_0	n
150	6.56×10^{-1}	3.5	1.3	6.4×10^{-9a}	2.5×10^{-9a}	0.6^a	-0.37^a
120	9.32×10^{-2}	25	1.3	4.1×10^{-9a}	3.8×10^{-10b}	0.6^b	-0.43^a
100	2.06×10^{-2}	125	1.3	2.7×10^{-9a}	8.4×10^{-11b}	0.6^a	-0.48^a

[a] Extrapolated
[b] Interpolated

diffusion consequently introduces no observable error. Slight discrepancies are, however, observed at the longer times at the highest temperatures, for which the predicted modulus at the centre of the sample continues to increase while the experimental data approach a maximum. Although the predictions shown at the lowest temperature (65°C) are all homogeneous, we expect that slight heterogeneities will develop at long times because the profiles are calculated as summations in time.

Figure 2 shows predicted profiles (solid curves) for the neoprene rubber, again treating all parameters as constants. Again, the agreement with experiment is excellent, especially at short times. The assumption of constant P_{ox} does slightly overestimate oxidation in the sample centres at long times at the lower temperatures. At 120°C, the data approach a maximum, but the predictions continue to increase. At 150°C, oxidation at the sample centre is predicted to reach a maximum, as observed in the data. The fact that the agreement for the neoprene is slightly worse than for the nitrile indicates that the permeability/modulus relation is stronger for the neoprene than for the nitrile.

Excellent quantitative agreement is obtained for the early stages of ageing for both materials. This agreement suggests that the permeability, which we assumed to be constant, in fact changes only slowly with modulus in the early stages of ageing. There are minor discrepancies between theory and experiment in the later stages of ageing. For most applications, however, this level of agreement is sufficient. As a practical matter, the ability to accurately model the profiles at long times is unnecessary because these materials typically exceed their useful service lifetimes before significant time-dependent effects develop. We previously showed[5] that maximum material lifetimes (defined as the normalized ultimate tensile elongation decreasing to ~0.05) correspond to the surface modulus increasing by approximately one order of magnitude. This corresponds to the early stages of ageing, before significant changes in P_{ox} occur. Thus, for predictions relevant to the service portion of the material lifetime, the assumption of constant P_{ox} is acceptable.

VARIABLE PERMEABILITY

The discrepancies between experimental and theoretical profiles obtained above (*Figures 1* and *2*) demonstrate that the assumption of constant P_{ox}, while adequate at short times, begins to break down at long times. We now extend the model so that P_{ox} varies with modulus to determine whether this effect can explain the discrepancies observed at longer times and, more generally, to determine the importance of this effect. Because the longer times are of little relevance to service lifetimes of the two materials discussed in this work, the discussion in this section is more of academic than practical significance for these materials.

Theory

There are two major differences between this analysis and the previous analysis in which P_{ox} remained constant. First, we need to determine appropriate functional forms for the permeability/modulus relationship as represented by its two components, the diffusivity/modulus and solubility/modulus relationships, given by α and β, respectively (equation (18)); and, second, we need to account for non-constant diffusivity and solubility in the continuity equation (equation (6)).

The distinction between permeability, diffusivity and solubility is expressed in the constitutive diffusion model. As mentioned earlier, we have, for this modelling, assumed Fickian diffusion, which refers implicitly to materials with constant solubility. This means that the solubility/modulus relationship is constant by assumption. This also means that any time dependencies must occur in the diffusivity/modulus relationship. Thus, we now develop a model in which diffusivity varies with modulus while solubility remains constant.

Under the assumption of constant solubility, the functional form of the solubility/modulus is again (equation (19)) the trivial identity

$$\beta_j(t) = \beta_0 \tag{23}$$

To determine an appropriate functional form for the diffusivity/modulus relationship, we begin by considering its theoretical basis so that we can justify extrapolation of the data. One approach is to use the Doolittle equation[14],

$$\ln \eta = B\left(\frac{v_0 - v}{v}\right) + \ln A \tag{24}$$

which models transport properties (e.g. viscosity, η) in elastomers as functions of free volume, v. The parameters A and B are material property constants. Because $D \propto 1/\eta$ (and, consequently, $P_{ox} \propto 1/\eta$), it can be argued from equation (24) that $D_j(t_i) \propto \exp(M_{j,i} - M_0)$ (see the Appendix), from which it follows that

$$\alpha_j(t_i) = \alpha_0 \exp[-b(M_{j,i} - M_0)] \tag{25}$$

The modulus range for which this equation is valid is unclear, however. Specifically, the Doolittle equation is intended to describe elastomers. Although the materials in this work are elastomers when unaged, they become heavily cross-linked (i.e. glassy) as they age. Other factors, such as the presence of fillers, may also affect the range of applicability. Thus, although we expect equation (25) to be valid for the early stages of ageing, we expect it to be invalid for the later stages of ageing.

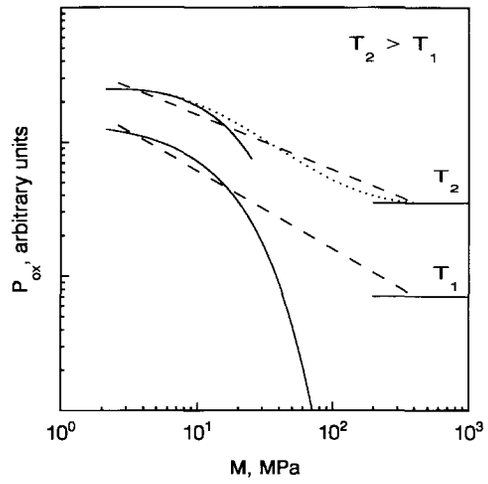

Figure 12 Expected theoretical behaviour of the permeability/modulus relation with increasing net cross-linking (modulus). Indicated modulus scale is approximately correct

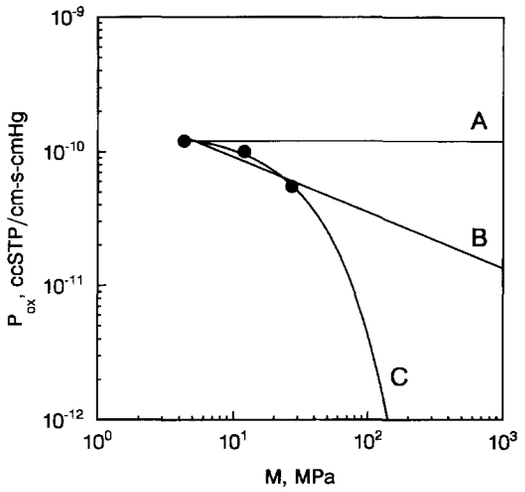

Figure 13 Oxygen permeability of the nitrile rubber as a function of modulus at 23°C. Indicated functional forms of P_{ox} vs. M are (A) constant, (B) power law and (C) exponential

As the material becomes increasingly cross-linked, it will behave as a glass, in which both permeability and diffusivity are relatively insensitive to modulus. Therefore, the behaviour of the diffusivity/modulus relation should be approximately as shown conceptually in *Figure 12*, decreasing exponentially in the low modulus range (solid curves) and approaching a constant in the high modulus range (solid horizontal lines). This means that, over the modulus range of interest, the diffusivity/modulus behaviour is probably described by a roughly (backwards) S-shaped curve (dotted curve), which can be well approximated by a power law functionality (dashed line):

$$\alpha_j(t_i) = \alpha_0\left(\frac{M_0}{M_{j,i}}\right)^n \tag{26}$$

where n is the power law slope. Recall that, for the early stages of ageing, we found the assumption of constant permeability to be adequate. This can be understood from *Figure 12*, which shows that the exponential dependence predicts only small changes in diffusivity (permeability) with modulus in the early stages of ageing. *Figure 13* shows the experimental permeability/modulus relationship for the nitrile rubber (solid circles) and three simple fits to the data (constant, power law and exponential). Notice that in *Figure 13* we have presented permeability/modulus data to support our discussion of the diffusivity/modulus relationship. Because it is easier for us to do so, we normally measure permeabilities rather than diffusivities. Under the assumption of constant solubility, however, these two parameters are constant multiples of each other and their mathematical treatments are equivalent.

It is often observed that the magnitudes of diffusivities and permeabilities are inversely related to the magnitudes of their respective activation energies[12,13,15]. That is, materials with low permeabilities tend to have high activation energies for permeability. This means that permeabilities will often display non-Arrhenius behaviour, as was observed in *Figures 6* and *10*. It therefore follows that the ratio of aged/unaged permeabilities will increase with temperature. That is, a given change in temperature will cause a larger change in the permeability of the aged material than in the permeability of the unaged material because the former has a lower absolute magnitude and thus changes more rapidly due to its higher activation energy. Similarly, for the transition from exponential (Doolittle) behaviour to 'constant' (glassy) behaviour, an increase in temperature causes the glassy permeability to increase more than the elastomeric permeability, with the result that the power law slope decreases (approaches zero) with increasing temperature (see *Figure 12*).

To modify the time-independent continuity equation to account explicitly for the case in which diffusivity varies with position within the sample, we use Fick's law with non-constant diffusivity:

$$\frac{\partial}{\partial x}\left(D\frac{\partial[O_2]}{\partial x}\right) = \frac{C_1[O_2]}{1 + C_2[O_2]} \tag{27}$$

which has the non-dimensional form

$$\frac{\partial^2\theta}{\partial X^2} + \frac{1}{D}\frac{\partial D}{\partial X}\frac{\partial\theta}{\partial X} = \frac{\alpha\theta}{1+\beta\theta} \tag{28}$$

Following the approach used to derive equation (8), and noting that

$$\left.\frac{\partial D}{\partial X}\right|_j = \frac{D_{j+1} - D_{j-1}}{2\delta X} \qquad \left.\frac{\partial\theta}{\partial X}\right|_j = \frac{\theta_{j+1} - \theta_{j-1}}{2\delta X} \tag{29}$$

we arrive at the following set of $k-1$ simultaneous equations as a solution to equation (28):

$$\theta_{j-1,i} = \left(\frac{1}{1-F_{j,i}}\right) \times \left(\frac{\alpha_{j,i}\theta_{j,i}(\delta X)^2}{1+\beta_0\theta_{j,i}} + 2\theta_{j,i} - \theta_{j+1,i} - F_{j,i}\theta_{j+1,i}\right) \tag{30}$$

with $j = 1, 2, 3, \ldots, k-1$ and

$$F_{j,i} = \frac{D_{j+1,i} - D_{j-1,i}}{4D_{j,i}} \tag{31}$$

Because S is constant by assumption, P_{ox} can be used instead of D in equation (31). When diffusivity is constant (i.e. $F_j = 0$ and, from equation (19), $\alpha_j = \alpha_0$), equation (30) the (numerical) solution to the continuity equation with non-constant diffusivity, reduces to equation (8), the (numerical) solution to the continuity equation with constant diffusivity.

Data

To calculate diffusivity (α) as a function of modulus (equation (18) or (26)), we begin by analysing the available permeability data. It is, of course, preferable to measure permeabilities only of homogeneously aged samples. This requirement imposes an upper limit on the permeability change that can easily be measured because at high temperatures (e.g. 125°C), for our nitrile samples of ~2 mm thickness, heterogeneities in the modulus profile develop before the modulus has doubled, while at low temperatures (e.g. 65°C) ageing occurs so slowly that the modulus, although homogeneous, increases only fourfold after 735 days. To obtain nitrile samples with significant changes in modulus, we are therefore forced to compromise and rely on measurements at intermediate temperatures. Even at the compromise temperature of 95°C, however, the delayed onset of heterogeneity limits the available range of homogeneous data. In this case, the maximum available change in modulus is approximately a factor of seven. In an attempt to obtain homogeneously aged samples with higher moduli, we used radiation ageing (^{60}Co). A sample of the nitrile rubber was aged 18 days at 35°C under inert conditions (argon), for a total radiation dose of 1.2 MGy.The aged sample had a homogeneous modulus of 39 MPa (factor of nine change in modulus) and had $P_{ox} = 1.0 \times 10^{-10}$ ccSTP cm^{-1} s^{-1} cmHg^{-1} at 23°C. Comparison to *Figure 6* or *13* shows that the permeability of this radiation-aged sample is considerably larger than expected for equivalent hardening resulting from thermal ageing. This indicates that non-oxidative cross-linking has a lesser effect on permeability than does oxidative cross-linking, the difference presumably resulting from incorporation of oxygen into the polymer matrix. Consequently, we were forced to rely solely on thermally aged samples, and some of the samples for which P_{ox} was measured were of necessity heterogeneous. It was therefore essential to understand how heterogeneity affects permeability.

To calculate an effective modulus (M_{eff}) of heterogeneous samples (at time t_i), we relate measured flux (J_i) to permeability and thus to modulus:

$$\frac{J_i}{J_0} = \frac{P_{ox_i}}{P_{ox_0}} \equiv q_{eff} \tag{32}$$

Constant flux through the sample implies

$$\frac{1}{q_{eff}} = \int_0^1 \frac{dX}{q} \simeq \sum_j \frac{X_j}{q_{j,i}} \tag{33}$$

where $q_{j,i}$ (and therefore $P_{ox_{j,i}}$) is related to $M_{j,i}$ through the power law (equation (26)). That is,

$$\frac{1}{q_{eff}} \simeq \sum_j X_j \left(\frac{M_0}{M_{j,i}}\right)^n \tag{34}$$

By combining average local values of $M_{j,i}$ corresponding to lengths X_j, both of which can be estimated from measured modulus profiles, n can easily be determined by trial and error by calculating the value of q_{eff} (equation (33) or (34)) that is consistent with measured fluxes J_i and J_0 (equation (32)). Once n is known, M_{eff} is calculated from equations (26) and (32) as

$$M_{eff} = M_0 \left(\frac{J_i}{J_0}\right)^{1/n} \tag{35}$$

Permeabilities were measured for three nitrile samples with different degrees of ageing. The unaged sample obviously had $M_{eff} = M_0 = 4.3$ MPa; a second sample, aged 149 days at 80°C, had $M_{eff} = 12$ MPa; a third sample, aged 84 days at 95°C, had $M_{eff} = 27$ MPa. The two aged nitrile samples were sufficiently homogeneous that the calculated values of M_{eff} were insensitive to n. *Figure 6* shows the permeation data as functions of temperature and effective modulus. We begin by considering only the permeation data at 23°C. By plotting these data as a function of modulus at room temperature, we eliminate the explicit time dependence and arrive at the results shown in *Figure 13*. Fitting these data to the power law functionality (equation (26)) (case B), we find $n \simeq -0.44$ at 23°C.

To determine how n varies with temperature, we introduce a parameter r,

$$r = \frac{P_{ox}(M_{eff})}{P_{ox}(M_0)} \tag{36}$$

to describe the behaviour of $P_{ox}(M_{eff})$ with temperature. Although the three data points for $M_{eff} = 27$ MPa in *Figure 6* could be interpreted to indicate that r is constant, close examination reveals that r increases from ~0.44 at 23°C to ~0.47 at 54°C to ~0.53 at 76°C. We extrapolated these data (lower curve in *Figure 6*) by treating r as Arrhenius ($E_a = 0.75$ kcal mol^{-1}) with respect to temperature (*Figure 14*). This temperature dependence of r is a natural result of the non-Arrhenius behaviour of P_{ox}. The power law exponent n is calculated (from only two data points) as

$$n(T) = \frac{\ln r(T)}{\ln(M_t/M_0)} = \frac{\ln r(T)}{\ln(27/4.3)} \tag{37}$$

The exponential parameter b (equation (25)) is calculated analogously:

$$b(T) = \frac{\ln r(T)}{M_t - M_0} = \frac{\ln r(T)}{27 - 4.3} \tag{38}$$

This analysis is detailed in *Figure 14*, in which the curves depicting n and b were calculated using equations (37) and (38), respectively. Note that b/n is a constant. Values of n and b used for the time-dependent modelling of the nitrile rubber are listed in *Table 2*.

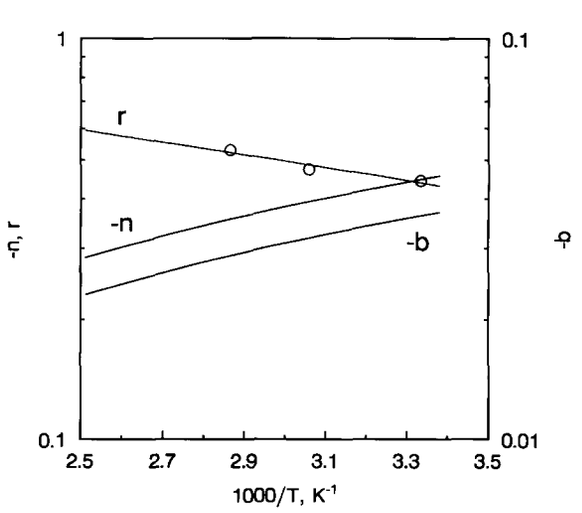

Figure 14 Analysis detailing temperature dependence of the parameters r, n and b for the nitrile rubber

The available permeability data for the neoprene rubber are shown in *Figure 10* as functions of temperature and effective modulus. All of the data relevant to quantification of the power law exponent are at 23°C and, due to incompatibilities between the physical size of the samples and the instrument with which we measure permeabilities, we cannot obtain any additional data. Determination of the temperature dependence of the power law exponent is thus somewhat problematic. Having no basis for calculating the activation energy for r for the neoprene, we assume it to be the same as that for r for the nitrile rubber, which we measured to be 0.75 kcal mol^{-1}. Due to the many similarities in behaviours of the two materials, we believe that this assumption is justifiable. We have measured, at 23°C, $r = 0.79$, 0.61 and 0.47 (corresponding to $n = -0.56$, -0.66 and -0.74) for three samples with $M_{eff} = 11$, 15.6 and 20 MPa, respectively. For predictions involving large changes in modulus, we calculate the power law exponent based on the most-aged data point ($M_{eff} = 20$ MPa), because it best represents a steeper power law appropriate to prediction of large changes in modulus. The lower curve in *Figure 10* shows the resulting extrapolation of r. The corresponding values of n used for the time-dependent modelling of the neoprene rubber are listed in *Table 3*.

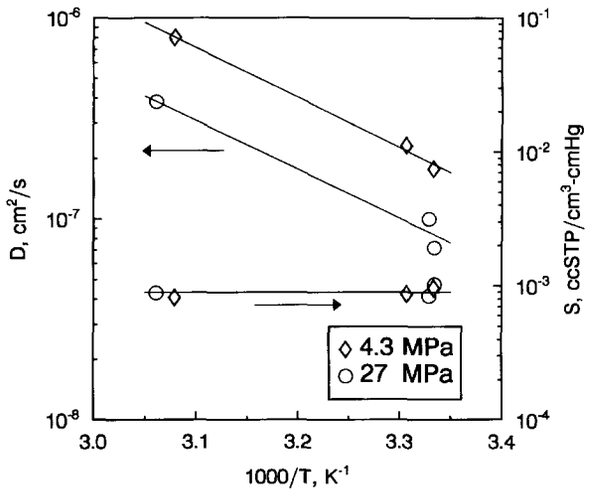

Figure 15 Oxygen diffusivity and solubility of the nitrile rubber as functions of temperature and ageing

Comparison with theory

We first review the available data to determine whether the assumption of constant solubility is valid for the nitrile rubber. When measuring permeabilities, diffusivities can be calculated from the lag time of the permeation response to a step change in oxygen concentration[16]. The solubility can then be calculated using the relation $P_{ox} = DS$. *Figure 15* shows the effect of ageing on D and S for the nitrile rubber. For this material, it is clear that S has essentially no time (or temperature) dependence. The same conclusion can be reached from the definition of β_0 ($= C_2Sp$, equation (4)) by noting that both β_0 (see *Figure 4*) and ϕ (see *Figure 3*), and therefore the oxidation kinetics represented in C_1 and C_2 (equation (2)), are time-independent. Having validated our assumption of constant solubility, we expect that the current model should be particularly appropriate for prediction of time-dependent profiles for the nitrile rubber.

Predictions of time-dependent profiles for the nitrile rubber when permeability changes with modulus according to the power law are shown in *Figure 16*. As for the case of assumed constant permeability (see *Figure 1*), the predictions at 65 and 80°C (not shown) are in excellent agreement with the data. At the higher temperatures at longer times, the predictions are, as expected, somewhat lower than those in *Figure 1*, but are still in good agreement with the data. At 125°C, the predicted modulus at the centre of the sample increases towards an asymptotic maximum, as do the data, eliminating the discrepancy observed when P_{ox} was assumed constant.

Predictions for the nitrile when permeability changes with modulus according to the Doolittle (exponential) law are shown in *Figure 17*. Again, the predictions at 65 and 80°C (not shown), as well as at short times at the higher temperatures, are in excellent agreement with the data. Indeed, the agreement for the early stages of ageing is arguably better in this case than for any other functional form of the permeability/modulus relation, indicating that the underlying (Doolittle) theory is probably correct. In the 95–125°C range, all relevant trends are predicted correctly, but the quantitative agreement near the edges shows some deviations: permeabilities decrease too rapidly in this model, with the result that predicted profiles are too steep near the edges. Even in this case of a strong permeability/modulus

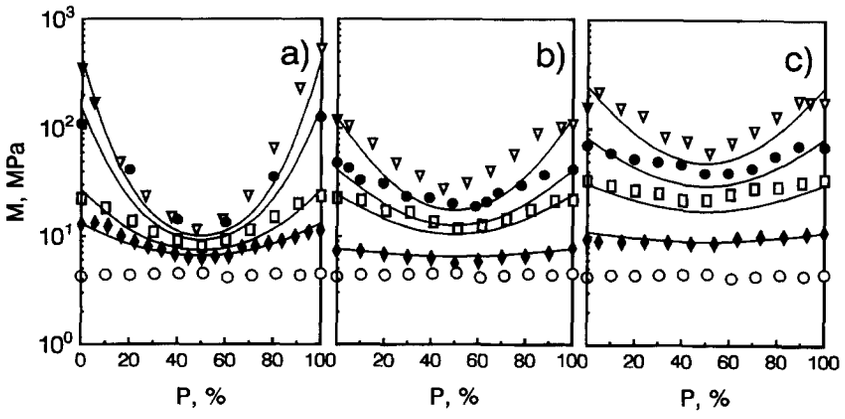

Figure 16 Predictions of time-dependent profiles for the nitrile rubber at (a) 125°C, (b) 110°C and (c) 95°C, assuming that the permeability/modulus relation is described by a power law (case B in *Figure 13*) where n varies with T. Symbol identification keys for the modulus data are given in *Figure 1*

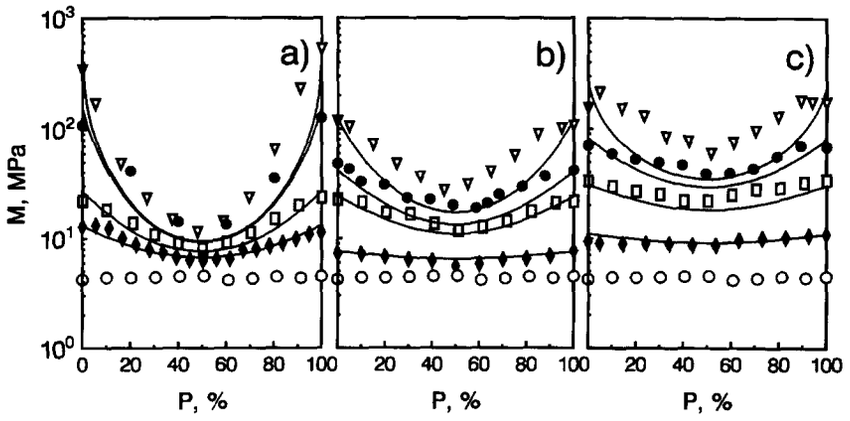

Figure 17 Predictions of time-dependent profiles for the nitrile rubber at (a) 125°C, (b) 110°C and (c) 95°C, assuming that the permeability/modulus relation is described by an exponential law (case C in *Figure 13*) where b varies with T. Symbol identification keys for the modulus data are given in *Figure 1*

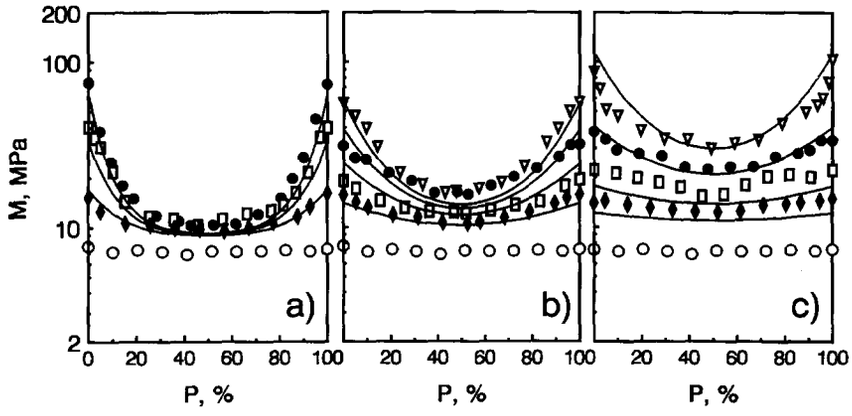

Figure 18 Predictions of time-dependent profiles for the neoprene rubber at (a) 150°C, (b) 120°C and (c) 100°C, assuming that the permeability/modulus relation is described by a power law where $n = -0.74$ (constant) based on $T = 23$°C. Symbol identification keys for the modulus data are given in *Figure 2*

dependence, however, agreement between theory and experiment is reasonable.

Predictions for the neoprene rubber when permeability changes with modulus according to the power law with $n = -0.74$, for $T = 23$°C, are shown in *Figure 18*. In this case, the predictions are all lower than the data, indicating that $n = -0.74$ is too severe a dependence for the permeability/modulus relationship. Because the data are bracketed by predictions based on $n = 0$ and $n = -0.74$, we conclude that $-0.74 < n < 0$, consistent with a temperature-dependent n.

Predictions for the neoprene when permeability changes with modulus according to the power law with a temperature-dependent n are shown in *Figure 19*. In this case, the predictions are in excellent agreement with the data in virtually all respects. One slight discrepancy is that the data near the edges for 123 days under the 100°C condition are somewhat steeper than the prediction; this discrepancy is not observed in the 75 day and earlier data. This may be due to severe edge hardening resulting from the increase in oxidation rate corresponding to the end of the induction period (~86 days at 100°C[5]). That is, after ~86 days, oxidation in the vicinity of the edges may become much more rapid than in the centre.

It is worth emphasizing that excellent quantitative agreement is obtained for the early stages of ageing, regardless of the functional form (constant, power law or exponential) chosen for the diffusivity/modulus relation. Similarly, even at long times, the predicted time-dependent behaviours are not especially sensitive to the functional form of the diffusivity/modulus relationship. That is, knowledge of the specific functional form of this relationship is not critical to successful modelling of time-dependent modulus profiles.

Variable solubility

In addition to changes in diffusivity, changes in permeability may also be due to changes in solubility. Rigorous treatment of such changes requires the use of a constitutive relation, e.g. Fick's law[10], for the flux that explicitly treats solubility as non-constant:

$$J = -D\left(\frac{dc}{dx} - D\frac{d\ln S}{dx}\right) \tag{39}$$

The fact that solubility and diffusivity have different functional dependences in equation (39) makes it difficult to determine *a priori* the relative magnitudes of their effects on the predicted profiles. But because only small chemical changes (approximately 1 oxidized site per 100 backbone carbon atoms) correspond to near-total degradations of elastomers, and because our results for

the earlier stages of degradation indicate only insignificant changes in solubility (see *Figure 15*), we expect solubility to be insensitive to modulus over the modulus regime of interest. If so, changes in solubility will have only a minor influence on the time-dependent predictions. We therefore choose not to pursue this line of inquiry.

OTHER ASPECTS OF THE MODELLING

The sensitivities of this modelling (assuming a power law dependence for the diffusivity/modulus relationship) to ϕ/P_{ox} (closely related to α_0, equation (3)), β_0 and n are shown in *Figure 20* for the nitrile rubber. These sensitivities refer to changes in the indicated parameter, with all other parameters held constant. Because diffusion limitations are most evident at high temperatures, we have chosen the 18 day at 125°C condition, which displays important diffusion-limited effects, as a reference point for comparison. (We showed earlier (see *Figures 1*, *16* and *17*) that diffusion limitations are not significant at lower temperatures and that the modelling is insensitive to the choice of functional form of the permeability/modulus relation.) In each of *Figures 20a*, *20b* and *20c*, the middle profile is the reference condition.

We believe that reasonable errors in the extrapolation from 95 to 125°C give $4.5 \times 10^{-9} < P_{ox} < 6.2 \times 10^{-9}$ and $1.0 \times 10^{-9} < \phi < 1.5 \times 10^{-9}$, so that $0.16 < \phi/P_{ox} < 0.30$, compared to the reference case, $\phi/P_{ox} = 0.21$ (see *Table 2*). As shown in *Figure 20a*, this uncertainty has a moderate quantitative effect (±25%) on the magnitude of the modulus predicted at the centre of the sample; qualitative agreements are unaffected. The excellent quantitative agreement shown in *Figures 1* and *16* indicates that our extrapolated values of ϕ and P_{ox} are likely correct. The sensitivity of the predicted profiles to β_0 is shown in *Figure 20b*. Profiles are virtually unchanged when β_0 is decreased by one order of magnitude; increasing β_0 by one order of magnitude causes drastic changes in the shape of the profile (formation of shoulders). Slight indications of shoulder formation are observed for the nitrile rubber at 95 and 110°C (see *Figure 1*). It is possible that these shoulders indicate that β_0 increases sharply in the later stages of ageing, although the available data (*Figure 5* and also the generally U-shaped experimental profiles, which suggest that $\beta_0 \sim 1$) argue against this interpretation. Finally, based on the small differences between the predicted profiles in *Figures 1* and *16*, we expect that sensitivity to the power law exponent n will be weak; this is indeed the case as shown in *Figure 20c*.

Long-term predictions for the nitrile rubber at intermediate and lower temperatures are shown in *Figure 21*. As expected, heterogeneities develop at the lower temperatures, but at increasingly long times. Additionally, the degree of heterogeneity decreases

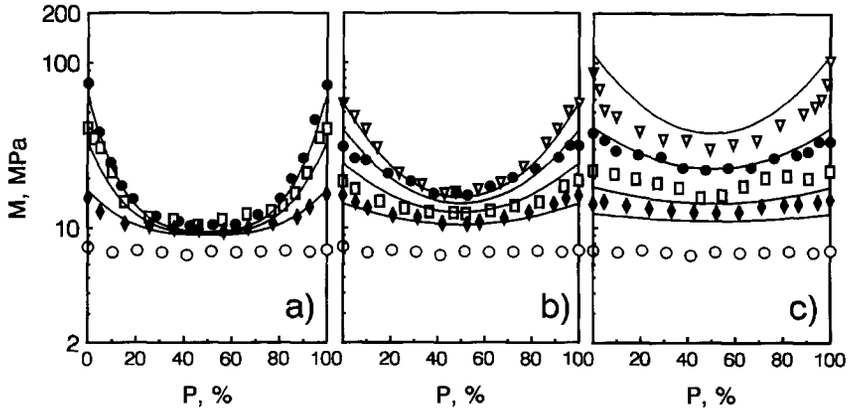

Figure 19 Predictions of time-dependent profiles for the neoprene rubber at (a) 150°C, (b) 120°C and (c) 100°C, assuming that the permeability/modulus relation is described by a power law where n varies with T. Symbol identification keys for the modulus data are given in *Figure 2*

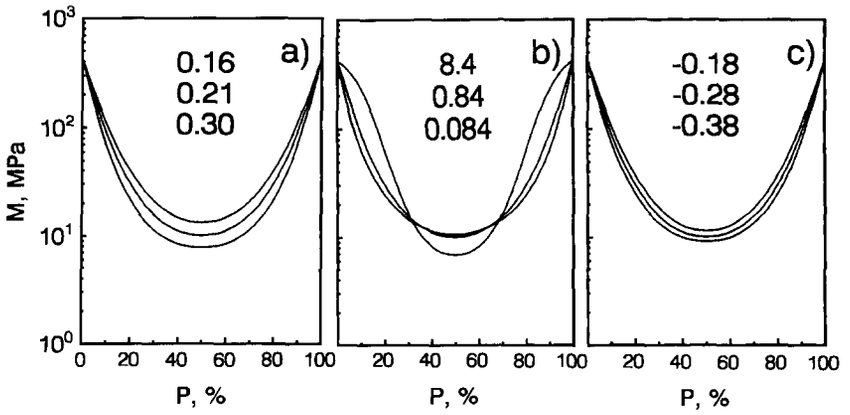

Figure 20 Sensitivities of the predicted nitrile rubber profile (18 days at 125°C (middle profile in each case)) for the indicated values of (a) ϕ/P_{ox}[=] mol cm Hg cmg^{-1} ccSTP^{-1}, (b) β_0 and (c) n

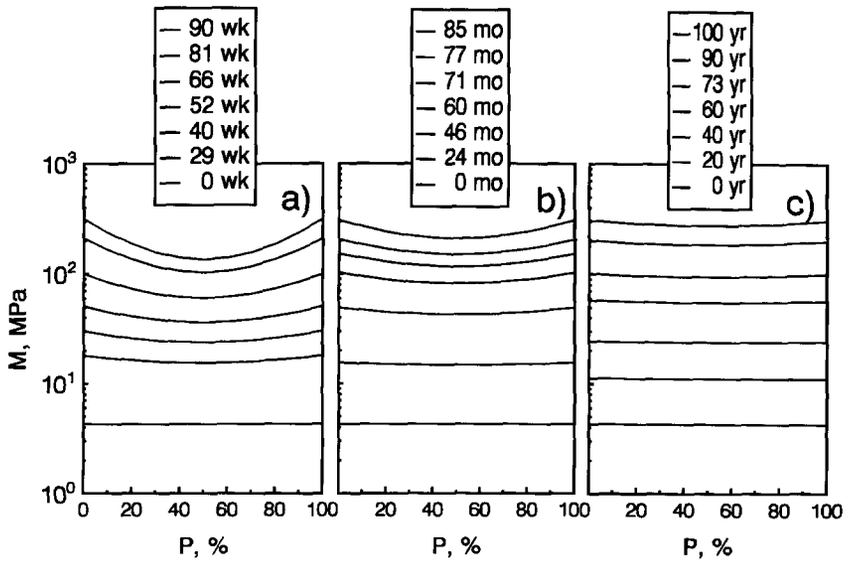

Figure 21 Long-term nitrile rubber ageing predictions at lower temperatures: (a) 80°C, (b) 65°C and (c) 40°C. In all cases, heterogeneous modulus profiles are predicted after sufficiently long times, although the degree of heterogeneity decreases as temperature decreases

with decreasing temperature. This effect is a direct result of the functional dependence of modulus on *cumulative* oxidation: Because the θ profile becomes increasingly homogeneous (smaller DLO effects) at lower temperatures, the cumulative heterogeneity is necessarily smaller than at higher temperatures.

It is common practice to estimate L_c, the critical sample thickness below which DLO effects are insignificant, from equation (3) as

$$L_c = \left(\frac{\alpha_c}{1+\beta_0}\frac{pP_{ox}}{\phi_0}\right)^{0.5} \tag{40}$$

where α_c is that value of α_0 for which the integrated oxidation across the sample is at least 90% of the homogeneously oxidized case. For thermal ageing of elastomers, we find $\beta_0 \sim 1$, a conclusion emphatically supported by the excellent agreement between experiment and theory in this work, which is based on $\beta_0 \sim 1$. When $\beta_0 \sim 1$, it follows that $\alpha_c/(1+\beta_0) \simeq 2$ (see *Figure 10* in Gillen and Clough[8]). However, equation (40) is frequently evaluated using $\alpha_c/(1+\beta_0) \simeq 8$[9,17], resulting in overestimation of L_c by a factor of 2.

SUMMARY AND CONCLUSIONS

We have developed a complete, quantitative model for the time development of DLO profiles and have demonstrated quantitative predictions of modulus profiles. Although developed explicitly for modulus profiles, we expect this treatment to be analogously applicable to modelling of other mechanical and also chemical properties. With the experimentally controllable parameters L and p and measurements of ϕ, β_0, P_{ox}, k_{air} and k_{nox}, the time-dependent profiles can be predicted with great accuracy and the extent of DLO assessed. For thermal ageing, β_0 can often be assumed to be near unity or can be well estimated with little effort from the shape of measured modulus profiles. Importantly, all parameters can be assumed constant (no time dependencies) for predictions relevant to the service lifetime of elastomers. Knowledge of the specific functional form of the permeability/modulus relationship is not critical to successful modelling of modulus profiles.

ACKNOWLEDGEMENTS

We thank G. M. Malone for able technical assistance. This work was performed at Sandia National Laboratories, supported by the US Department of Energy under Contract No. DE-AC04-94AL85000.

REFERENCES

1 Gillen, K. T., Clough, R. L. and Quintana, C. A. *Polym. Degrad. Stabil.* 1987, **17**, 31
2 Gillen, K. T. and Clough, R. L. *Polym. Eng. Sci.* 1989, **29**, 29
3 Clough, R. L. and Gillen, K. T. *Polym. Degrad. Stabil.* 1992, **38**, 47
4 Smith, J. M. 'Chemical Engineering Kinetics', 2nd edn, McGraw-Hill, New York, 1970, Ch. 12
5 Wise, J., Gillen, K. T. and Clough, R. L. *Polym. Degrad. Stabil.* 1995, **49**, 403
6 Bolland, J. L. *Proc. R. Soc.* 1946, **A186**, 218
7 Bateman, L. *Q. Rev. Chem. Soc.* 1954, **8**, 147
8 Gillen, K. T. and Clough, R. L. *Polymer* 1992, **33**, 4358
9 Cunliffe, A. V. and Davis, A. *Polym. Degrad. Stabil.* 1982, **4**, 17
10 Higuchi, A. and Nakagawa, T. *J. Polym. Sci., Polym. Phys. Ed.* 1990, **28**, 2247
11 Barrer, R. M. and Skirrow, G. *J. Polym. Sci.* 1948, **3**, 549
12 Van Amerongen, G. J. *J. Polym. Sci.* 1950, **5**, 307
13 Kosiyanon, R. and McGregor, R. *J. Appl. Polym. Sci.* 1981, **26**, 629
14 Doolittle, A. K. and Doolittle, D. B. *J. Appl. Phys.* 1957, **28**, 901
15 Van Amerongen, G. J. *Rubber Chem. Technol.* 1964, **37**, 1065
16 Pauly, S. *Radiat. Phys. Chem.* 1992, **39**, 269
17 Seguchi, T., Hashimoto, S., Arakawa, K., Hayakawa, N., Kawakami, W. and Kuriyama, I. *Radiat. Phys. Chem.* 1981, **17**, 195

APPENDIX. PERMEABILITY/FREE VOLUME RELATIONSHIP

Noting that $D \propto 1/\eta$ allows us to rewrite equation (24) as

$$\ln\frac{D_v}{D_{v_0}} = B\left(\frac{1}{v_0} - \frac{1}{v}\right) \tag{A1}$$

We expect that free volume v will change with cross-link density ν as

$$v = v_0 - k\Delta\nu \tag{A2}$$

where $\Delta\nu$, the change in cross-link density, is given by

$$\Delta\nu = \nu - \nu_0 = \frac{1}{m_c} - \frac{1}{m_{c_0}}$$
$$\propto M_i - M_0 = \Delta M \tag{A3}$$

Equation (A3) assumes that both free volume and modulus are proportional to the reciprocal of the molecular weight between cross-links, m_c. Thus,

$$v = v_0 - k'\Delta M \tag{A4}$$

and equation (A1) can be rewritten as

$$\ln\frac{D_v}{D_{v_0}} = B\left(\frac{1}{v_0} - \frac{1}{v_0 - k\Delta M}\right) \tag{A5}$$

We assume that small changes in free volume account for the changes in P_{ox}; that is,

$$\frac{k\,\Delta\nu}{v_0} = \frac{k'\Delta M}{v_0} \ll 1 \tag{A6}$$

Under the assumption given in equation (A6), it follows that

$$\frac{1}{v_0 - k'\Delta M} = \frac{1}{v_0(1 - k'\Delta M/v_0)} \cong \frac{1}{v_0}\left(1 + \frac{k'\Delta M}{v_0}\right) \tag{A7}$$

which allows equation (A5) to be rewritten as

$$\ln\frac{D_v}{D_{v_0}} = -\frac{B}{v_0^2}k'\Delta M = b\,\Delta M \tag{A8}$$

That is,

$$D_j(t_i) \propto \exp[b(M_{j,i} - M_0)] \tag{A9}$$